THE JOURNAL OF BIOLOGICAL CHEMISTRY
Vol. 274, No. 27, Issue of July 2, pp. 19048–19054, 1999

Printed in U.S.A.

Oxidizing Side of the Cyanobacterial Photosystem I

EVIDENCE FOR INTERACTION BETWEEN THE ELECTRON DONOR PROTEINS AND A LUMINAL SURFACE HELIX OF THE PsaB SUBUNIT*

(Received for publication, October 13, 1998, and in revised form, April 7, 1999)

Jun Sun‡, Wu Xu‡, Manuel Hervás§, José A. Navarro§, Miguel A. De La Rosa§, and Parag R. Chitnis‡¶

From the ‡Department of Biochemistry and Biophysics, Iowa State University, Ames, Iowa 50011 and the §Instituto de Bioquímica Vegetal y Fotosíntesis, Universidad de Sevilla y Consejo Superior de Investigaciones Científicas, 41092 Sevilla, Spain

Photosystem I (PSI) interacts with plastocyanin or cytochrome c_6 on the luminal side. To identify sites of interaction between plastocyanin/cytochrome c_6 and the PSI core, site-directed mutations were generated in the luminal J loop of the PsaB protein from *Synechocystis* sp. PCC 6803. The eight mutant strains differed in their photoautotrophic growth. Western blotting with subunit-specific antibodies indicated that the mutations affected the PSI level in the thylakoid membranes. PSI proteins could not be detected in the S600R/G601C/N602I, N609K/S610C/T611I, and M614I/G615C/W616A mutant membranes. The other mutant strains contained different levels of PSI proteins. Among the mutant strains that contained PSI proteins, the H595C/L596I, Q627H/L628C/I629S, and N638C/N639S mutants showed similar levels of PSI-mediated electron transfer activity when either cytochrome c_6 or an artificial electron donor was used. In contrast, cytochrome c_6 could not function as an electron donor to the W622C/A623R mutant, even though the PSI activity mediated by an artificial electron donor was detected in this mutant. Thus, the W622C/A623R mutation affected the interaction of the PSI complex with cytochrome c_6. Biotin-maleimide modification of the mutant PSI complexes indicated that His-595, Trp-622, Leu-628, Tyr-632, and Asn-638 in wild-type PsaB may be exposed on the surface of the PSI complex. The results presented here demonstrate the role of an extramembrane loop of a PSI core protein in the interaction with soluble electron donor proteins.

Photosystem I (PSI)[1] is a multisubunit membrane-protein complex that catalyzes electron transfer from the reduced plastocyanin in the thylakoid lumen to the oxidized ferredoxin in the chloroplast stroma or cyanobacterial cytoplasm (1–4). In cyanobacteria and green algae, cytochrome c_6 can substitute plastocyanin depending on the growth conditions (5–7). The crystal structure of PSI at 4-Å resolution is available (8, 9). PSI contains 89 chlorophyll *a* molecules, 83 of which constitute the core antenna system. The PsaA and PsaB subunits form the heterodimeric core that harbors most of the antenna chlorophyll *a* molecules, β-carotenes, the primary electron donor P700, and a chain of electron acceptors (A_0, A_1, and F_X). In addition to the core proteins, the cyanobacterial PSI complex contains three peripheral proteins (PsaC, PsaD, and PsaE) and six integral membrane proteins (PsaF, PsaI, PsaJ, PsaK, PsaL, and PsaM) (1–3). The PsaC, PsaD, and PsaE subunits constitute the reducing side of the PSI complex. PsaC binds the terminal electron acceptors F_A and F_B, which donate electrons to ferredoxin. PsaD and PsaE facilitate the docking of ferredoxin on PSI (1). Functions of the other subunits have been studied by using subunit-deficient mutants of cyanobacteria and algae (10–17).

On the luminal side of thylakoid membranes, PSI accepts electrons from plastocyanin or cytochrome c_6. The interaction of plastocyanin with plant and algal PSI complexes shows a fast kinetic step, which can be attributed to a multistep reaction mechanism of electron transfer (18, 19). Some cyanobacteria have a simpler one-step bimolecular collision mechanism (20, 21). Cross-linking studies have indicated that plastocyanin can be cross-linked to the N-terminal lysine-rich region of chloroplast PsaF, which is not found in cyanobacterial PsaF (22). Thus, the interaction between plastocyanin and plant PSI includes initial electrostatic interactions between the N-terminal domain of PsaF and the conserved negative patches of plastocyanin. However, the PsaF subunit of PSI is not required in the interaction with plastocyanin in *Synechocystis* sp. PCC 6803 (13, 14, 23) and in *Synechococcus elongatus* (24). The deletion of PsaF in *Chlamydomonas reinhardtii* did not abolish the electron transfer from plastocyanin to P700 (25). Therefore, plastocyanin and cytochrome c_6 contact the PsaA and PsaB core proteins directly. The luminal extramembrane loops of PsaA and PsaB are likely candidates for interaction with plastocyanin during electron transfer.

In the crystal structure of PSI, the luminal side of PSI is flat with a 10-Å protrusion beyond the membrane boundary (8, 9). There is a 3-nm deep indentation in the center, perhaps caused by a partial separation between PsaA and PsaB. In the structural modeling, the dimensions of plastocyanin matched well inside this cavity (26, 27). Near the luminal indentation, the two surface α-helices *l* and *l′* are parallel to the membrane plane and are located near the P700 chlorophyll *a* dimer (8, 9). The *l* and *l′* helices are analogous to similar surface helices in the purple bacterial reaction center (26, 28). The *l* and *l′* helices are in the extramembrane J loops that are located between the

* This work was supported in part by United States Department of Agriculture-National Research Initiative Competitive Grants Program Grant 97-35306-4555, European Union Grants CHRX-CT94-0540 and FMRX-CT98-0218, and Spanish Ministry of Education and Science Grant PB96-1381. This is Journal Paper J-18118 of the Iowa Agriculture and Home Economics Experiment Station (Ames, IA), Project 3416, supported by Hatch Act and State of Iowa funds. The costs of publication of this article were defrayed in part by the payment of page charges. This article must therefore be hereby marked "*advertisement*" in accordance with 18 U.S.C. Section 1734 solely to indicate this fact.

¶ To whom correspondence should be addressed. Tel.: 515-294-1657; Fax: 515-294-0453; E-mail: chitnis@iastate.edu.

[1] The abbreviations used are: PSI and PSII, photosystems I and II, respectively; DM, dodecyl β-D-maltoside; WT, wild-type; RWT, recovered wild-type; PAGE, polyacrylamide gel electrophoresis; DAD, 3,6-diaminodurene; MV, methyl viologen; Tricine, *N*-[2-hydroxy-1,1-bis(hydroxymethyl)ethyl]glycine.

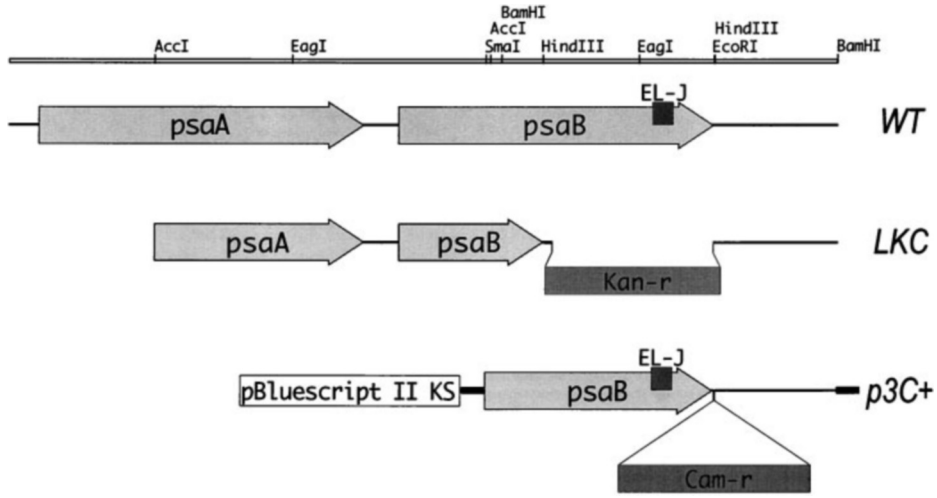

FIG. 1. **Generation of PsaB mutants.** The restriction map of the *Synechocystis* sp. PCC 6803 genomic region around the *psaA* and *psaB* genes is shown on the *top line. Arrows* show the location, size, and direction of complete or partial *psaA* and *psaB* genes. The *small black boxes* indicate the coding region for the extramembrane J loop (*EL-J*) of PsaB. The kanamycin resistance gene (*Kan-r*) and the chloramphenicol resistance gene (*Cam-r*) are shown as *long boxes*. The *bold lines* in the construction of the p3C$^+$ plasmid represent the pBluescript II KS vector.

transmembrane *k* and *m* helices of the core proteins (see Ref. 29 for the topology of PSI core proteins and nomenclature of loops). We postulate that these helices interact with plastocyanin during electron transfer.

To investigate the role of the J loops in the assembly and function of the PSI complex and in the interaction with the electron donors, we generated cysteine-scanning multipoint mutations in conserved amino acids in the J loop of the PsaB protein. A residue was changed to a cysteinyl residue in each of the mutations. Such an approach has been used to study the topographical features of membrane proteins (30, 31). The mutations were introduced into a *psaB* deletion strain of *Synechocystis* sp. PCC 6803. Here we present the biochemical characterization of the mutant strains.

EXPERIMENTAL PROCEDURES

Cyanobacterial Cultures, Membrane Isolation, and PSI Purification—Strains of *Synechocystis* sp. PCC 6803 were cultured in BG-11 medium with appropriate antibiotics (30 mg/liter chloramphenicol or 40 mg/liter kanamycin) at 30 °C. For autotrophic growth, cells were grown in BG-11 medium under medium light intensity of 40 μmol·m^{-2}·s^{-1}. For heterotrophic growth, cells were grown in BG-11 supplemented with 5 mM glucose under low light intensity of 5 μmol·m^{-2}·s^{-1}. Cells were harvested at the late exponential growth phase. Previously published methods were used for isolation of thylakoid membranes and purification of trimeric PSI complexes with DM (32). The chlorophyll *a* concentration (33) and the carotene concentration (34) were estimated according to previously published methods.

Generation of Mutations in the psaB Gene—For mutagenesis in the C-terminal region of the PsaB protein of *Synechocystis* sp. PCC 6803, a PSI-less recipient strain (LKC) was generated by replacing a 1187-base pair 3′-coding region of the *psaB* gene (the *Hin*dIII–*Eco*RI fragment) with a cassette for kanamycin resistance (Fig. 1). For this purpose, we constructed a plasmid that contained the kanamycin resistance gene cassette and an 843-base pair 3′-flanking region downstream of the *psaB* gene. Upstream from the resistance cartridge, the plasmid contained a 2703-base pair *Acc*I–*Hin*dIII fragment that includes most of the *psaA* gene, the 5′-region of the *psaB* gene, and the untranslated region between the *psaA* and *psaB* genes. The plasmid was introduced into a PSI-less strain, which has a partial deletion of *psaA* and *psaB* genes and is capable of heterotrophic growth under low light intensity (35, 36). The resulting kanamycin-resistant recipient strain is capable of heterotrophic growth under low light intensity. To introduce the WT and mutant *psaB* genes into the recipient strain, we constructed the p3C$^+$ recombinant plasmid. In this plasmid, a 1587-base pair *Sma*I–*Eco*RI fragment of the *psaB* gene (including the 3′-coding region of *psaB*), a chloramphenicol resistance gene, and the 3′-flanking region were cloned into the polylinker of pBluescript II KS (Stratagene) (Fig. 1). All PsaB mutants were generated by a polymerase chain reaction-mediated mutation technique (37). The mutagenic oligonucleotide primers contained a *Pst*I or an *Nsi*I restriction endonuclease recognition site. The mutated recombinant plasmids were sequenced completely to ensure the presence of desired changes and the absence of errors by *Taq* DNA polymerase. The DNAs were used to transform the recipient strain LKC. The p3C$^+$ plasmid with the WT gene was introduced back into the LKC strain to yield the recovered wild-type (RWT) strain that was used as the positive control in these studies. The transformation was performed at 30 °C under heterotrophic growth conditions as described (38). The chloramphenicol-resistant transformants were selected, segregated for three generations, and replica-plated to confirm the absence of the kanamycin resistance gene.

Characterization of the Mutant Strains—After segregation, the chloramphenicol-resistant transformants were cultured in liquid BG-11 medium, and the genomic DNA was isolated. Integration of the chloramphenicol resistance gene into the genome of the mutant strains was confirmed by polymerase chain reaction amplification of appropriate fragments using genomic DNA. The nucleotide sequence of the corresponding polymerase chain reaction fragments was determined to confirm mutations. Cell counting showed that number of cells per $A_{730\ nm}$ is the same (5.5×10^7 cells·$A_{730\ nm}{}^{-1}$·ml^{-1}) for both the RWT and LKC cultures. $A_{730\ nm}$ was measured using a UV-160U spectrophotometer (Shimadzu, Tokyo, Japan) and was used as a measure of cell count to monitor the growth of the mutant strains and in normalizing other characteristics of the mutant strains. Accumulation of PSI proteins was examined by analytical SDS-PAGE and immunodetection (29). The antibodies that were used for immunodetection have been described previously (32). The P700 content was estimated by the measurement of photoinduced absorbance changes at 820 nm (20, 39). The mutant PSI complexes were modified by biotin-maleimide according to a previously published method (32).

The PSII activity of *Synechocystis* cells was measured as light-driven oxygen evolution in which electrons are transferred from water to *p*-benzoquinone via the PSII complex. The PSI activity was monitored by oxygen uptake with the Mehler reaction (40, 41) using the artificial electron carriers DAD and MV (32). In this reaction, ascorbate reduces DAD, which in turn donates electrons to P700. Light-driven PSI electron transfer reduces MV. The oxidation of the reduced MV consumes oxygen. Alternatively, the PSI activity in the membrane can be measured by oxygen uptake with 15 μM cytochrome c_6 replacing DAD as the electron donor. The PSI activity in the membrane was also determined from NADP$^+$ photoreduction assays using cytochrome c_6 and ferredoxin as the electron donor and acceptor of the PSI complex, respectively (32). These activities were normalized on an equal cell basis.

RESULTS

Mutagenesis of the J Loop of the PsaB Protein—In the crystal structure of the PSI complex, a pair of surface helices (*l* and *l*′) are present in the extramembrane J loops. The secondary structure prediction using the Garnier algorithm (42) indicated a putative α-helix in the J loop of PsaB from Met-614 to Tyr-632 (Fig. 2). This peptide fragment is highly conserved among the PsaB proteins from higher plants, algae, and cyanobacteria. This region also shows high homology between the PsaA and PsaB proteins. Besides the putative helix, several other amino acid residues in the J loop are also conserved among PsaB

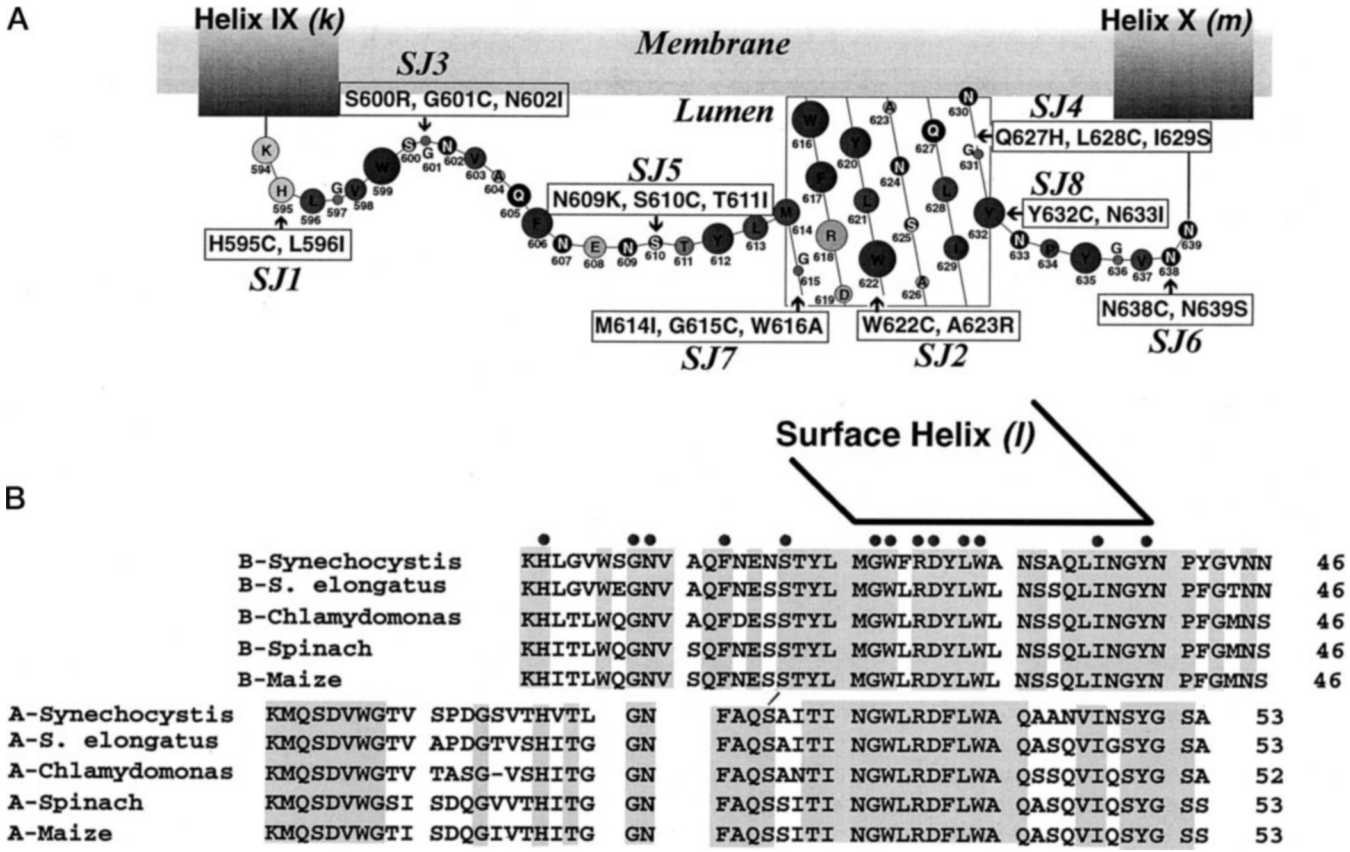

FIG. 2. **Mutagenesis of the J loop of the PsaB protein.** *A*, folding model for the extramembrane J loop of PsaB. Amino acids are indicated and numbered for the PsaB protein of *Synechocystis* sp. PCC 6803. The surface helix is represented as a *box* with the predicted sequence aligned inside. The positions and identities of the mutations are indicated. *B*, comparison of the primary sequences of the J loop of PsaB and PsaA from different sources. The completely conserved residues among species are *shaded. Dots* indicate the residues that are conserved between PsaA and PsaB.

proteins from different sources and between the PsaA and PsaB proteins. We targeted these conserved residues in the mutagenesis experiments and generated eight multipoint mutations in the J loop of the PsaB protein (Fig. 2).

Characterization of the Mutant Cells—The PSI-less LKC cells were more blue than the WT cells due to the reduced level of chlorophyll while retaining phycobilisomes (36). During segregation, the RWT strain as well as the SJ1, SJ2, SJ4, SJ6, and SJ8 mutant strains formed green colonies, whereas the SJ3, SJ5, and SJ7 mutant strains formed bluish colonies that resembled the recipient LKC strain.

The RWT, LKC, and mutant strains were cultured under photoautotrophic and heterotrophic growth conditions, and the increase in cell density was measured (Table I). All strains grew heterotrophically with similar doubling time, ranging from 27 to 30 h, indicating their similar abilities to utilize externally supplied glucose under low light intensity. Therefore, the respiratory system was not affected in the mutant strains. Under photoautotrophic growth conditions, cells of the LKC, SJ3, SJ5, SJ7, and SJ8 strains either died or did not grow. The RWT and SJ6 cells had the fastest growth, whereas the SJ1, SJ2, and SJ4 cells grew slower than the RWT cells. Therefore, all mutations, except for the amino acid replacements in SJ6, affected the autotrophic growth of the mutant strain. These differences in the autotrophic growth rates could result from the effects of mutations on the photosynthetic activity.

The chlorophyll and carotene contents of these strains were measured using the cells that had been grown under heterotrophic conditions (Table I). The LKC cells had the lowest content, whereas the RWT cells contained the highest content of these pigments. Among the mutant strains, the bluish SJ3, SJ5, and SJ7 strains had relatively low chlorophyll and carotene content, whereas the other strains showed higher chlorophyll/cell and carotene/cell ratios. Therefore, the color of the mutant cells correlates to their pigment content, which in turn may reflect the change of the abundance of the pigment-binding proteins. The strains that were able to grow photoautotrophically were green strains containing relatively high pigment content. Thus, the mutations might affect the photosystem complexes, which are the major pigment-binding proteins.

The impact of mutations on the photosystem activity in the mutant strains was studied by oxygen measurement. The PSII and PSI activities in the intact cells were measured by oxygen evolution and uptake with the artificial electron carriers, respectively (Table I). The photosynthetic activities were normalized on an equal cell basis. The PSII activity of the 10 strains ranged from 576 to 787 nmol of $O_2 \cdot A_{730\ nm}{}^{-1} \cdot h^{-1}$, which was 84–114% of the RWT level. Therefore, the PSII activity was not affected substantially by the mutations in the PsaB protein. As expected, the PSI-less LKC strain contained no PSI activity, whereas the RWT cells had an activity of −237 nmol of $O_2 \cdot A_{730\ nm}{}^{-1} \cdot h^{-1}$. The lack of PSI activity in the SJ3, SJ5, and SJ7 mutant strains was consistent with their inability to grow autotrophically. The SJ8 mutant strain contained only 8% of the RWT activity, which might not be sufficient for autotrophic growth. The SJ1, SJ2, SJ4, and SJ6 mutant strains showed different levels of PSI activity with various autotrophic growth rates. The changes of PSI activity in the mutant strains may

TABLE I
Characterization of the mutant cells

Strains	Doubling time		Pigment content		Photosynthetic activity	
	Heterotrophic	Autotrophic	Chlorophyll	Carotene	PSII	PSI
	h		$\mu g \cdot A_{730\,nm}^{-1} \cdot ml^{-1}$		$nmol\ O_2 \cdot A_{730\,nm}^{-1} \cdot h^{-1}$	
LKC	30	—[a]	0.73	0.32	576	0
RWT	27	54	1.29	0.83	688	−237
SJ1	27	70	1.19	0.79	685	−260
SJ2	27	81	0.99	0.63	743	−89
SJ3	28	—	0.85	0.45	668	−4
SJ4	27	172	1.02	0.72	787	−62
SJ5	28	—	0.75	0.39	692	0
SJ6	27	54	1.04	0.70	686	−124
SJ7	28	—	0.88	0.44	727	−5
SJ8	28	—	0.89	0.55	730	−19

[a] —, these strains died or did not grow.

result from the effect of the mutations on the assembly and/or function of PSI. To test these possibilities, we examined the accumulation and function of the PSI complexes in the thylakoid membranes.

Accumulation of PSI Proteins in the Mutant Membranes—PsaB is an integral membrane protein with 11 transmembrane helices. Mutations in the PsaB protein could disturb protein folding and affect the assembly of the PSI complex. We performed Western blotting to estimate the steady-state levels of PSI proteins in the membranes. Thylakoid membranes were isolated from mutant strains, and their proteins were resolved by SDS-PAGE. Immunodetection was performed with polyclonal antibodies against PsaA, PsaB, PsaC, PsaF, PsaI, PsaK, or PsaL (Fig. 3). The results were consistent on all seven Western blots. As expected, no PSI protein was detected in the LKC membranes, whereas the RWT membranes contained PSI proteins. PSI proteins were not detected in SJ3, SJ5, and SJ7 membranes, consistent with the lack of PSI activity in these cells. Therefore, the SJ3, SJ5, and SJ7 mutations abolished the accumulation of PSI proteins in the membrane. The absence of PSI proteins in the SJ3, SJ5, and SJ7 mutants resulted in their inability to grow autotrophically and the blue color of the cells. PSI proteins were detected in the SJ1, SJ2, SJ4, SJ6, and SJ8 mutants at varying levels that were less than the RWT level. Therefore, the mutations in the SJ1, SJ2, SJ4, SJ6, and SJ8 strains allowed some accumulation of PSI proteins in the membrane. To study the effect of mutations on the photosynthetic function of the accumulated PSI complexes, the SJ1, SJ2, SJ4, SJ6, and SJ8 mutant membranes were subjected to functional analysis.

Photosynthetic Characterization of the Mutant Membranes—The active P700 reaction centers in the intact thylakoid membranes were measured by laser-induced changes in the absorbance at 820 nm and were normalized on an equal cell basis (Table II). The active P700 reaction centers in the DM extracts were also measured to investigate the stability of the reaction centers (Table II). The PSI photosynthetic activity was determined with different sets of electron donors and acceptors: DAD/MV, cytochrome c_6/MV, and cytochrome c_6/ferredoxin. The DAD/MV PSI activity, which was measured by oxygen uptake with an excess of the artificial electron donor (DAD) and acceptor (MV), excludes the limitation by interprotein recognition and docking on both sides of the membrane and therefore indicates the efficiency of electron transfer within the PSI complex. When cytochrome c_6 replaces DAD as the electron donor of PSI in the oxygen uptake measurements, the cytochrome c_6/MV PSI activity reflects both the electron transfer rate within the PSI complex and the interaction between cytochrome c_6 and the PSI complex. The PSI-mediated $NADP^+$ photoreduction uses cytochrome c_6 and ferredoxin as the electron donor and acceptor, respectively. Thus, the cytochrome c_6/ferredoxin PSI activity includes the electron transfer activity and the interaction between the PSI complex and the soluble proteins on both sides of the membrane. The difference between the DAD/MV and the cytochrome c_6/MV PSI activities indicates an impact on the interaction between the PSI complex and cytochrome c_6. Similarly, the difference between the cytochrome c_6/MV and the cytochrome c_6/ferredoxin PSI activities indicates the effect on the interaction between the PSI complex and ferredoxin. In all mutant membranes, the cytochrome c_6/MV and the cytochrome c_6/ferredoxin PSI activities were at a similar percentage of the RWT level. Thus, the mutations on the luminal loop did not affect the interaction between the PSI complex and ferredoxin on the cytoplasmic side.

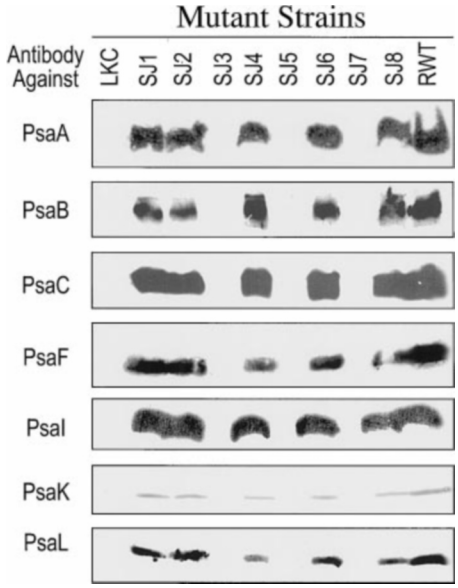

FIG. 3. **Accumulation of the PSI proteins in the mutant strains.** Membranes were analyzed by Tricine/urea/SDS-PAGE and Western blotting with subunit-specific antibodies. The immunodetection was visualized by enhanced chemiluminescence.

The SJ1 and SJ6 mutations were located in the two ends of the J loop. These two mutants had higher autotrophic growth rates than the other mutants. They both contained active P700 and cytochrome c_6/MV PSI activity at the same percentage of the RWT level. However, 41% active P700 in the intact membrane of the SJ1 mutant was lost after DM extraction. Therefore, the P700 reaction centers of the SJ1 mutant were labile to detergent extraction, suggesting an impact of the mutation on the packing of helices in the membrane. We reported earlier

TABLE II

Characterization of the mutant photosynthetic membranes

The results were normalized on an equal cell basis and are expressed as a percentage of the RWT level that is shown in parentheses. The level of P700 in the DM extract is expressed as a percentage of the RWT level in the membrane.

Strains	Level of active P700		PSI photosynthetic activity		
	Membrane	DM extract	DAD/MV	Cytochrome c_6/MV	Cytochrome c_6/ferredoxin
			$nmol \cdot A_{730\,nm}^{-1} \cdot h^{-1}$		
RWT	100 (6.91×10^4 P700/cell)	95	100 (−237)	100 (−326)	100 (49)
SJ1	44	26	110	44	58
SJ2	29	29	38	0	0
SJ4	23	26	26	23	28
SJ6	45	35	52	44	56
SJ8	10	8	8	0	0

that proteolysis of the extramembrane loops facilitates the access of the small artificial electron carriers to the electron transfer centers in the PSI complex, resulting in an increase in the DAD/MV PSI activity (29). The SJ1 mutation might change the packing of the transmembrane *k* helix that is adjacent to the P700 reaction center, which may favor the access of small DAD molecules to the P700 reaction center. Consistent with this postulate, we observed high DAD/MV PSI activity in the SJ1 mutant. Similarly, the SJ6 mutant also lost 22% active P700 reaction centers upon DM extraction. With less loss of active P700, the SJ6 mutant did not show such a dramatic increase in the DAD/MV PSI activity as the SJ1 mutant. The SJ6 mutation may have less impact on the packing of transmembrane helices than the SJ1 mutation. In summary, the SJ1 and SJ6 mutations affected the accumulation of PSI proteins in the membrane and the packing of helices around P700, but did not interrupt the interaction between the PSI complex and cytochrome c_6.

The SJ2, SJ4, and SJ8 mutations were located in the middle of the J loop. These mutants grew slowly or did not grow under autotrophic growth conditions. Upon extraction by DM, the SJ2, SJ4, and SJ8 extracts maintained a similar level of active P700 reaction centers as in their intact membranes. Therefore, the SJ2, SJ4, and SJ8 mutations did not affect the conformation around the P700 reaction center. Among them, the SJ4 mutant contained similar levels of active P700, DAD/MV PSI activity, and cytochrome c_6/MV PSI activity, which were about one-fourth of the RWT level. Therefore, the SJ4 mutation decreased greatly the accumulation of PSI proteins in the membrane, but did not affect the interaction of the PSI complex with cytochrome c_6. In contrast, the SJ2 mutant contained 29% active P700 and 38% DAD/MV PSI activity of the RWT level, but neither cytochrome c_6/MV nor cytochrome c_6/ferredoxin electron transfer activity was detected in the SJ2 mutant membranes. Therefore, the SJ2 mutation affected the interaction between the PSI complex and cytochrome c_6. It reduced the accumulation of PSI complexes, but did not affect the conformation around P700. The slow autotrophic growth of the SJ2 mutant in the absence of cytochrome c_6-mediated PSI activity may be due to the electron transfer from plastocyanin or a third electron donor as indicated in an earlier study (43). Similar to the SJ2 mutant, the SJ8 mutant membrane contained no cytochrome c_6/MV PSI activity, even though active P700 and the DAD/MV PSI activity were detected in the SJ8 mutant. Therefore, the SJ8 mutation greatly decreased the accumulation of the PSI complexes and might have interrupted the interaction of the PSI complex with cytochrome c_6.

Modification of Mutant PSI Complexes—The PsaA and PsaB proteins in the WT complexes could not be modified by biotin-maleimide (Fig. 4), which specifically reacts with the sulfhydryl group of cysteinyl residues. Therefore, the cysteinyl residues of the WT PsaA and PsaB proteins were not exposed on the surface of PSI complexes. To study the topology of the J loop, we changed one amino acid to a cysteinyl residue in each of the eight mutations. PSI complexes from the SJ1, SJ2, SJ4, SJ6, SJ8, and RWT strains were purified and treated with biotin-maleimide. The biotin-maleimide-treated PSI complexes were resolved by Tricine/urea/SDS-PAGE, probed with peroxidase-conjugated avidin, and then developed with enhanced chemiluminescence reagents (Fig. 4). WT PsaAB could not be modified by biotin-maleimide. When the WT PSI complexes were incubated with SDS to denature the proteins, we could detect modification of the PsaAB proteins by biotin-maleimide. A small amount of RWT PsaAB proteins was labeled by biotin-maleimide, which might be due to partial unfolding in a small fraction of the PSI complexes during the preparation. The SJ1, SJ2, SJ4, SJ6, and SJ8 PSI complexes were modified by biotin-maleimide. Therefore, the cysteinyl residues introduced in these strains were exposed on the surface, suggesting that the corresponding residues in the WT PsaB protein (His-595, Trp-622, Leu-628, Tyr-632, and Asn-638) may be exposed on the surface of the PSI complex.

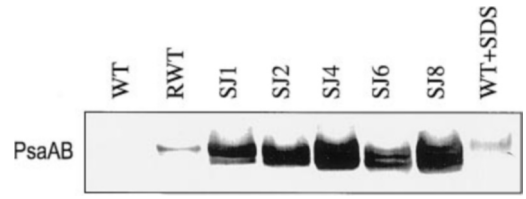

FIG. 4. **Modification of the mutant PSI complexes.** Purified PSI complexes containing 5 μg of chlorophyll were treated with biotin-maleimide and analyzed by Tricine/urea/SDS-PAGE. The blot was probed with peroxidase-conjugated avidin and visualized by enhanced chemiluminescence reagents.

To study the effect of the biotin-maleimide modification on PSI function, the cytochrome c_6/ferredoxin PSI activity was measured after the modification and expressed as a percentage of the RWT level. The cytochrome c_6/ferredoxin activities of modified PSI complexes from mutant strains were reduced substantially from their levels before modification. SJ1 was reduced from 58 to 34%, SJ4 was reduced from 28 to 11%, and SJ6 was reduced from 56 to 26% of the activity of the modified RWT membranes. Therefore, the modification of residues in the J loop by biotin-maleimide may interfere with the interaction of the PSI complex with the electron donor cytochrome c_6, providing further support for an interaction between the exposed surface of the J loop and cytochrome c_6.

DISCUSSION

The PSI complex accepts electrons from plastocyanin or cytochrome c_6 on the luminal side of the thylakoid membrane.

Examination of the structures of plastocyanin and cytochrome c_6 revealed the presence of a flat hydrophobic surface around the redox center in both proteins (44, 45). These flat hydrophobic surfaces are essential for the electron transfer from plastocyanin or cytochrome c_6 to PSI (12, 46). Correct hydrophobic interactions are expected to ensure the accurate orientation of plastocyanin or cytochrome c_6 on the PSI complex. Therefore, the two surface α-helices *l* and *l*′ and other amino acid residues in the J loops of the core proteins might provide the site for interaction with plastocyanin or cytochrome c_6. We tested this hypothesis by generating mutations in the J loop of PsaB.

Replacement of conserved residues in the J loop affected levels of PSI proteins in the membranes to varying degrees. The decreased accumulation of PSI proteins in the mutant membranes could result from several factors. A mutation might disturb the assembly of the mutant PsaB protein into the thylakoid membrane or cause a rapid turnover of the mutant PsaB protein. The mutation might affect the interaction between PsaB and other PSI subunits and result in fast degradation of PSI complexes. Since the deletion of PsaF, PsaL, PsaI, and PsaJ subunits did not affect the accumulation of PsaA and PsaB proteins (14, 16, 17, 47), the decreased accumulation of PSI proteins in the mutant strains is likely due to the decreased accumulation of the PsaB protein. The SJ3, SJ5, and SJ7 mutants did not allow accumulation of detectable levels of PSI proteins in the membranes. These mutations are located in the region between Ser-600 and Trp-616. Therefore, this peptide fragment is important for the stability of the PsaB protein in the membrane. Biotin-maleimide modification of the SJ1, SJ2, SJ4, SJ6, and SJ8 PSI complexes indicated that His-595, Trp-622, Leu-628, Tyr-632, and Asn-638 in WT PsaB might be exposed on the surface of the PSI complex. Mutations of the surface-exposed residues had a less destabilizing effect on the PsaB protein than the changes in the buried residues. For this reason, we propose that the *l* helix is exposed on the surface of the J loop, whereas the peptide fragment from Ser-600 to Trp-616 may fold underneath the helix.

Upon extraction by DM, the SJ1 and SJ6 mutants lost some active P700 reaction centers, suggesting an impact of mutations on the packing of transmembrane helices around P700. Other mutants maintained their active P700 after detergent extraction. The SJ1 and SJ6 mutations are located in the ends of J loop and close to the ends of the transmembrane *k* and *m* helices. Therefore, the amino acid residues at the junction of the transmembrane helix and extramembrane loop might be important for the packing of transmembrane helices.

The SJ2, SJ4, and SJ8 mutations were predicted to be located in the *l* helix. When we viewed the *l* helix as a wheel diagram, Trp-622, Leu-628, and Tyr-632 were aligned on one side of the helical wheel that is largely hydrophobic. These residues were determined exposed to solvent in the WT PSI complex (Fig. 4). This hydrophobic side of the *l* helix, containing Trp-622, Leu-628, and Tyr-632, may provide a surface for the hydrophobic interaction with plastocyanin/cytochrome c_6. The SJ2 and SJ8 membranes contained no cytochrome c_6/MV and cytochrome c_6/ferredoxin PSI activities, but maintained DAD/MV PSI activity. Therefore, the SJ2 and SJ8 mutations maintained electron transfer activity, but failed in interacting with cytochrome c_6. The SJ2 and SJ8 mutants maintained their active P700 reaction centers upon detergent extraction, indicating no impact on the conformation around P700 by the mutations. Therefore, the observed interruption of the PSI interaction with cytochrome c_6 in the SJ2 and SJ8 mutants is likely due to the amino acid replacement. In each of these two mutants, a large aromatic residue was replaced with the smaller cysteinyl residue. In contrast, the SJ4 membrane maintained similar levels of PSI proteins, active P700, and PSI activities and did not interrupt the interaction between the PSI complex and cytochrome c_6. In the SJ4 mutation, a leucinyl residue was changed to a cysteinyl residue. However, when the SJ4 PSI complexes were modified by biotin-maleimide with dramatic structural change, the PSI $NADP^+$ photoreduction activity was reduced substantially. The physical structure of the hydrophobic side of the *l* helix is important for the interaction of the PSI complex with cytochrome c_6. Therefore, our results show that the hydrophobic side of the *l* helix of the PsaB protein that contains Trp-622, Leu-628, and Tyr-632 provides the site of interaction with cytochrome c_6.

Acknowledgments—We thank Dr. Wim F. J. Vermaas for the initial PSI-less strain that contains a partial deletion of the *psaA* and *psaB* genes and Dr. John H. Golbeck for antibodies against the PsaC, PsaD, and PsaE subunits. We also thank Dr. Donald A. Heck and T. Wade Johnson for critically reading the manuscript.

REFERENCES

1. Chitnis, P. R. (1996) *Plant Physiol.* (*Bethesda*) **111,** 661–669
2. Fromme, P. (1996) *Curr. Opin. Struct. Biol.* **6,** 473–484
3. Chitnis, P. R., Xu, Q., Chitnis, V. P., and Nechushtai, R. (1995) *Photosynth. Res.* **44,** 23–40
4. Golbeck, J. H. (1994) in *The Molecular Biology of Cyanobacteria* (Bryant, D. A., ed) pp. 179–220, Kluwer Academic Publishers Group, Dordrecht, The Netherlands
5. Wood, P. M. (1978) *Eur. J. Biochem.* **87,** 9–19
6. Sandmann, G. (1986) *Arch. Microbiol.* **145,** 76–79
7. Kerfeld, C. A., and Krogmann, D. W. (1998) *Annu. Rev. Plant Physiol. Plant Mol. Biol.* **49,** 397–425
8. Krauß, N., Schubert, W.-D., Klukas, O., Fromme, P., Witt, H. T., and Saenger, W. (1996) *Nat. Struct. Biol.* **3,** 965–973
9. Schubert, W.-D., Klukas, O., Krauß, N., Saenger, W., Fromme, P., and Witt, H. T. (1997) *J. Mol. Biol.* **272,** 741–769
10. Wynn, R. M., Luong, C., and Malkin, R. (1989) *Plant Physiol.* (*Bethesda*) **91,** 445–449
11. Hippler, M., Ratajczak, R., and Haehnel, W. (1989) *FEBS Lett.* **250,** 280–284
12. Haehnel, W., Jansen, T., Gause, K., Klosgen, R. B., Stahl, B., Michl, D., Huvermann, B., Karas, M., and Herrmann, R. G. (1994) *EMBO J.* **13,** 1028–1038
13. Chitnis, P. R., Purvis, D., and Nelson, N. (1991) *J. Biol. Chem.* **266,** 20146–20151
14. Xu, Q., Yu, L., Chitnis, V. P., and Chitnis, P. R. (1994) *J. Biol. Chem.* **269,** 3205–3211
15. Chitnis, V. P., and Chitnis, P. R. (1993) *FEBS Lett.* **336,** 330–334
16. Xu, Q., Hoppe, D., Chitnis, V. P., Odom, W. R., Guikema, J. A., and Chitnis, P. R. (1995) *J. Biol. Chem.* **270,** 16243–16250
17. Xu, Q., Odom, W. R., Guikema, J. A., Chitnis, V. P., and Chitnis, P. R. (1994) *Plant Mol. Biol.* **26,** 291–302
18. Haehnel, W., Propper, A., and Krause, H. (1980) *Biochim. Biophys. Acta* **593,** 384–399
19. Bottin, H., and Mathis, P. (1985) *Biochemistry* **24,** 6453–6460
20. Hervas, M., Navarro, J. A., Diaz, A., Bottin, H., and De la Rosa, M. A. (1995) *Biochemistry* **34,** 11321–11326
21. Hervas, M., Navarro, J. A., Diaz, A., and De la Rosa, M. A. (1996) *Biochemistry* **35,** 2693–2698
22. Hippler, M., Reichert, J., Sutter, M., Zak, E., Altschmied, L., Schröer, U., Herrmann, R. G., and Haehnel, W. (1996) *EMBO J.* **15,** 6374–6384
23. Xu, Q., Jung, Y. S., Chitnis, V. P., Guikema, J. A., Golbeck, J. H., and Chitnis, P. R. (1994) *J. Biol. Chem.* **269,** 21512–21518
24. Hatanaka, H., Sonoike, K., Hirano, M., and Katoh, S. (1993) *Biochim. Biophys. Acta* **1141,** 45–51
25. Farah, J., Rappaport, F., Choquet, Y., Joliot, P., and Rochaix, J. D. (1995) *EMBO J.* **14,** 4976–4984
26. Fromme, P., Schubert, W.-D., and Krauss, N. (1994) *Biochim. Biophys. Acta* **1187,** 99–105
27. Boekema, E. J., Boonstra, A. F., Dekker, J. P., and Rögner, M. (1994) *J. Bioenerg. Biomembr.* **26,** 17–29
28. Deisenhofer, J., and Michel, H. (1991) *Annu. Rev. Cell Biol.* **7,** 1–23
29. Sun, J., Xu, Q., Chitnis, V. P., Jin, P., and Chitnis, P. R. (1997) *J. Biol. Chem.* **272,** 21793–21802
30. Altenbach, C., Flitsch, S. L., Khorana, H. G., and Hubbell, W. L. (1989) *Biochemistry* **28,** 7806–7812
31. He, M. M., Sun, J., and Kaback, H. R. (1996) *Biochemistry* **35,** 12909–12914
32. Sun, J., Ke, A., Jin, P., Chitnis, V. P., and Chitnis, P. R. (1998) *Methods Enzymol.* **297,** 124–139
33. Arnon, D. (1949) *Plant Physiol.* (*Bethesda*) **24,** 1–14
34. Furr, H. C., Barua, A. B., and Olson, J. A. (1992) in *Modern Chromatographic Analysis of Vitamins* (Leenheer, A. P. D., Lambert, W. E., and Nelis, H. J., eds) pp. 1–71, Marcel Dekker, Inc., New York
35. Boussiba, S., and Vermaas, W. F. J. (1992) in *Research in Photosynthesis* (Murata, N., ed) Vol. III, pp. 429–432, Kluwer Academic Publishers Group, Dordrecht, The Netherlands
36. Shen, G., Boussiba, S., and Vermaas, W. F. (1993) *Plant Cell* **5,** 1853–1863
37. Higuchi, R. (1989) in *PCR Technology* (Erlich, H. A., ed) pp. 61–70, Stockton Press, New York

38. Williams, J. G. K. (1988) *Methods Enzymol.* **167,** 766–778
39. Mathis, P., and Setif, P. (1981) *Isr. J. Chem.* **21,** 316–320
40. Mehler, A. H. (1951) *Arch. Biochem. Biophys.* **33,** 65–77
41. Mehler, A. H. (1951) *Arch. Biochem. Biophys.* **34,** 339–351
42. Garnier, J., Osguthorpe, D. J., and Robson, B. (1978) *J. Mol. Biol.* **120,** 97–120
43. Zhang, L., Pakrasi, H. B., and Whitmarsh, J. (1994) *J. Biol. Chem.* **269,** 5036–5042
44. Navarro, J. A., Hervas, M., and De la Rosa, M. A. (1997) *J. Biol. Inorg. Chem.* **2,** 11–12
45. Frazao, C., Soares, C. M., Carrondo, M. A., Pohl, E., Dauter, Z., Wilson, K. S., Hervas, M., Navarroo, J. A., De la Rosa, M. A., and Sheldrick, G. M. (1995) *Structure* **3,** 1159–1169
46. Sigfridsson, K., Young, S., and Hansson, O. (1996) *Biochemistry* **35,** 1249–1257
47. Chitnis, V. P., Xu, Q., Yu, L., Golbeck, J. H., Nakamoto, H., Xie, D. L., and Chitnis, P. R. (1993) *J. Biol. Chem.* **268,** 11678–11684